

Field study of wave attenuation on an offshore coral reef

Thomas A. Hardy

Department of Civil and Systems Engineering, James Cook University, Townsville, Queensland, Australia

Ian R. Young

Department of Civil Engineering, University College, University of New South Wales, Canberra
Australian Capital Territory, Australia

Abstract. A major field experiment was conducted which obtained measurements of the attenuation and transformation of short gravity waves as they cross the windward edge of an offshore coral reef. Water level data were collected for over 3000 individual time series during a wide range of environmental conditions. At the innermost measurement site, which is located on the horizontal reef flat after the completion of wave breaking, the upper bound of significant and maximum wave heights is limited to less than 40% and 60% of the reef flat water depth, respectively. As with significant wave height, both the shape and energy level of the reef flat spectra are strongly affected by changes in reef flat water depth. For higher tide levels the spectra on the reef flat closely mimic the corresponding incident spectra. However, the attenuation is greater for both lower frequencies and higher-energy portions of the spectra. This causes the reef flat spectra to be broader than those measured windward of the reef. At lower water levels, considerable energy losses due to wave breaking and bottom friction occur. Most of the energy loss comes from the vicinity of the spectral peak, and energy shifts to harmonics of the peak of the spectrum can be seen.

1. Introduction

A characteristic of shallow water in many tropical and some subtropical regions is the presence of coral reefs. Energy dissipation processes which occur at the seaward edges of these reefs and the subsequent spectral transformations as waves propagate across shallow reef flats are important in the prediction of wave conditions leeward of such regions. The morphology of coral reefs is very different from that of beaches, the environment in which almost all of the studies of the interaction of waves and shallow water have been conducted. Unlike beaches, which often have a relatively gently sloping bottom, coral reefs can present an almost vertical transition from relatively deep to very shallow water.

The Great Barrier Reef (GBR) dominates the wave climate along the northeastern coast of Australia (Figure 1). Contrary to its name, the GBR, for much of its length, is far from a continuous barrier. Instead it is composed of over 2600 individual reefs that are spread in both the alongshore and cross-shelf directions. Since this porous barrier is sometimes as much as 100 km from the mainland coast, the prediction of the wave climate in the GBR region presents a unique challenge. Wave information is needed, not only along the mainland coast and in the GBR lagoon (the region between the reef and the mainland), but also inside the complex matrix of reefs.

Unlike mainland beach and fringing reef-lagoon systems, where waves terminate and their energy is dissipated or transformed into water level change and current, waves can propagate across offshore coral reefs without complete dissi-

pation. Significant amounts of wave energy can pass out the leeward edges of offshore reefs, especially at higher tide levels. On windward reef flats, dissipation and transformations occur over a very short length scale compared with that of the much longer and deeper fetches on either side of the reef flat. The fieldwork presented in this paper is seen as a first step in the development of a modeling system for the prediction of waves in offshore reef regions. In this paper we will maintain our analyses in the frequency domain in order to provide information for the determination of techniques to calculate the attenuation and transformation of wave spectra in the reef surf zone. In the future this will allow easier coupling, in frequency domain, with wave generation modeling which is necessary both windward and leeward of the reef fronts. Thus we will focus on the transformation of wave spectra rather than switch to a wave-by-wave approach, as is often used in mainland surf zones.

To overcome the lack of data in the offshore reef environment, a major field experiment was conducted to measure the attenuation of waves across an offshore coral reef flat. To the authors' knowledge, the field experiment was the first to measure waves on the windward reef flat of an offshore coral reef.

This work is divided into the following three areas: (1) the collection of field data, (2) the analysis of the field data, and (3) the incorporation of the data into a simple and practical numerical model of the transformation of wave spectra over coral reef flats. Only the first two of these are reported in this paper. The numerical modeling will be reported separately. Investigating the complex nonlinear interactions of waves and reefs using higher-order modeling (e.g., Boussinesq) and the development of a combined wave generation and reef flat wave modeling system for the entire GBR region are topics of ongoing and future research.

Copyright 1996 by the American Geophysical Union.

Paper number 96JC00202.
0148-0227/96/96JC-00202\$09.00

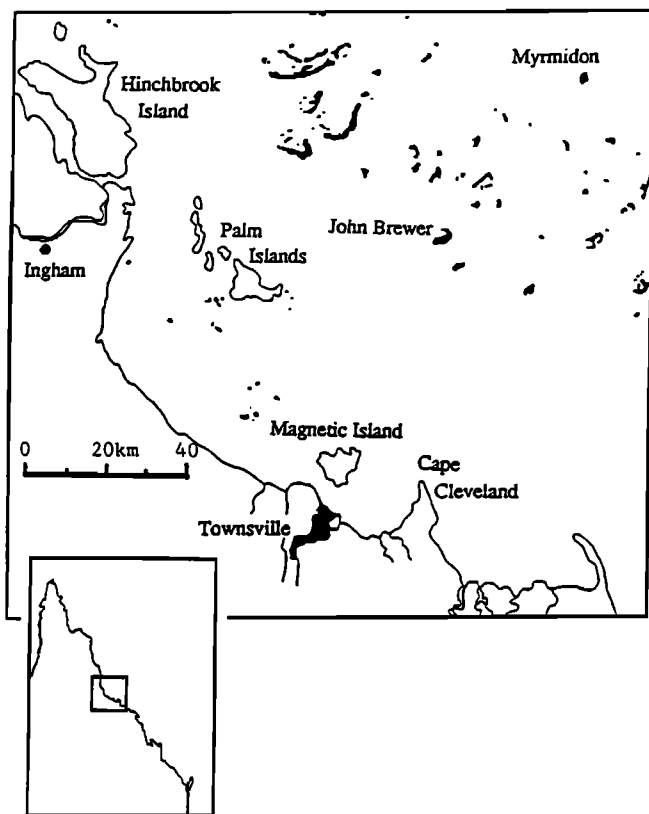


Figure 1. The northeast coast of Australia and the Great Barrier Reef.

2. Review of Literature

The most comprehensively reported field experiment of waves on coral reefs was the Ala Moana Experiment, which was conducted on the south coast of the island of Oahu in Hawaii during 1976. This experiment was reported in *Black* [1978], *Lee and Black* [1979], and *Gerritsen* [1981a, b]. Waves and water levels were measured along a linear transect normal to the bathymetric contours.

This study has several limitations in the investigation of wave-reef interactions. A total of only eight time series, each approximately 1 hour in duration, was collected. Data represent only a small range of water levels and wave conditions. The difference between the highest and lowest water levels was 0.36 m. The significant wave heights at the outermost station ranged from 0.5 to 0.85 m. The incident waves were dominated by swell with wave periods between 12 and 18 s. The slope of the bottom just seaward of the reef front is relatively gradual compared with many other coral reefs. Finally, the Ala Moana Reef is a fringing reef (a coral reef located in close proximity to the mainland or a large continental island).

Several field studies, which have measured wave attenuation over fringing reefs, have been undertaken in the Caribbean. *Roberts et al.* [1975, 1977] measured significant changes in spectra after wave breaking over a reef crest. Almost all of the energy loss occurred from near the peak frequency, and little energy was lost at higher frequencies. Thus the spectra from measurements in the reef lagoon were flatter and broader than those from measurements seaward of the reef crest.

Another report [*Roberts*, 1981] on field studies on fringing reefs, gives similar results - large attenuation across the reef

crest and broad, flat spectra landward of the reef crest. *Lugo-Fernandez* [1989] reports substantial energy dissipation, both across the reef front (65% reduction from forereef energy) and across the reef flat (75% reduction from forereef values). The spectra progressively broaden as the waves travel across the reef front and the reef flat.

Both field and laboratory studies of wave attenuation over a fringing reef were reported by *Kono and Tsukayama* [1980]. The reef flat spectra varied with the tidal level. At high tide the reef flat spectra had peaks at the second and third harmonics.

The authors are aware of only one previous field study on an offshore coral reef. That work [*Young*, 1989] in the ribbon reefs in the far northern section of the GBR was the preliminary study for that which is reported in this paper. Three wave measuring instruments were deployed on a transect normal to the reef front for a month long data collection period. The main conclusions of the experiment were the following: Wave attenuation was a function of both reef flat water depth and incident wave height. There was a distinctive flattening and broadening of the wave spectra after the waves passed over the reef flat. On the basis of satellite data, it appeared that the downstream influence of an isolated reef was much broader than the projected area of the reef. Finally, there was no evidence of wave reflection from the almost vertical seaward reef front.

Several other papers report on wave-reef interaction studies but do not discuss wave attenuation. These include *Munk and Sargent* [1948]; *Inman et al.* [1963]; *Tait* [1972]; *Seelig* [1983]; and *Jensen* [1991] all of whom report on field, laboratory, or analytic studies to determine the wave effects on water levels in fringing reef lagoons.

As would be expected, the above studies report a large dissipation in wave energy as waves abruptly encounter the very shallow water of a coral reef flat. Significantly, several of the studies report a broadening of the wave spectra, as will be confirmed in the present study. However, all of the study results suffer from deficiencies, and none adequately defines the characteristics of wave transformation on an offshore coral reef. To address these deficiencies, the field study and data analyses seek to study wave attenuation for reefs which are characterized by the following: (1) offshore rather than fringing reefs, (2) step-like reef fronts with almost vertical transitions from relatively deep to shallow water, (3) incident wave conditions that resemble sea rather than swell, and (4) a large tidal range.

3. Field Experiment

John Brewer Reef, located 70 km northeast of Townsville, Queensland, Australia in the central section of the GBR (Figure 1) was selected as the site for the field experiment. Site selection was based primarily on logistics. John Brewer Reef had a daily tourist catamaran service from Townsville, as well as a permanent accommodation facility in the form of a floating hotel. It would have been difficult, if not impossible, to conduct the experiment without the availability of transport and a safe and stable accommodation base.

The central section of the Great Barrier Reef is one of the least densely reefed segments of the GBR. John Brewer Reef is on the inner (landward) edge of the reef matrix and is elliptical in shape, with approximate dimensions of 6 km by 3 km (Figure 2), with the major axis approximately normal to the predominant southeasterly wind direction.

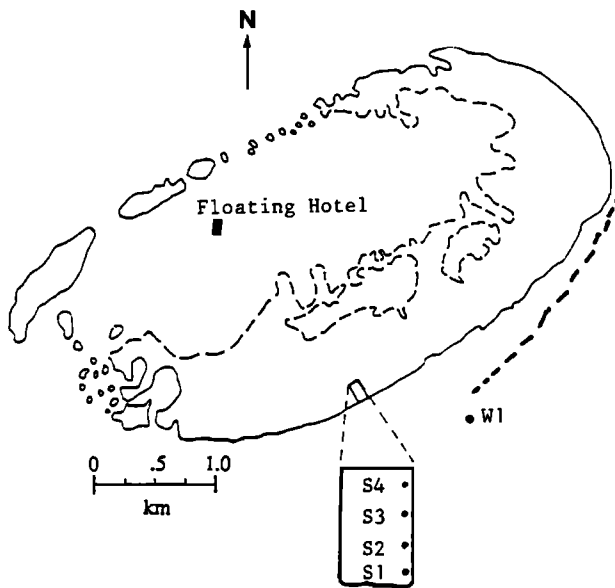


Figure 2. Plan view of John Brewer Reef with instrument locations.

The regional weather patterns are typically controlled by large high-pressure systems which move to the east, just south of the Australian continent, and into the Tasman Sea, which separates Australia and New Zealand. Tight pressure gradients between the high-pressure systems to the south and lower pressure to the north of the study region can cause strong and persistent winds (up to 25 to 35 knots (13 to 18 m s^{-1})). The lower end of this range of wind speeds occurs several times each year, and episodes can last for several days. These winds, which usually have directions between south and east are the strongest winds encountered outside of tropical cyclones.

The astronomical tides at Townsville are semidiurnal with a diurnal inequality. Highest astronomical tide (HAT) is 3.73 m low water datum (LWD). Lowest astronomical tide (LAT) is -0.28 m (LWD) and the mean spring range is approximately 2.34 m. The tidal range at John Brewer Reef is approximately 90% of the range at Townsville.

A coral ridge or "false front" (shown as a dashed line in Figure 2) lies just off the windward side of John Brewer Reef. It attaches to the main reef at the northeast corner and stretches about two-thirds of the way down the windward side, approximately 200 m from the main reef front. The ridge is relatively narrow, 10-20 m wide, and the depth of the top varies from 2 to 20 m below LAT. The seabed surrounding the reef drops rapidly to a fairly constant elevation of approximately 50 m below LAT.

The windward edge of the reef is a continuous reef flat that is 200 to 300 m wide and uniform in elevation at approximately 0.1 m above LAT. This reef flat not only extends along the southeastern edge but also wraps around both the southwestern and northeastern ends of the reef, extending along a total of approximately three-fifths of the perimeter of the reef. The reef flat is composed of coarse sand and small to medium pieces of coral rubble, which are mostly less than 0.2 m in diameter. There are occasional live coral heads or dead coral remnants with diameters of the order of 1 m, which sit on the reef flat and protrude above the water surface at lower water levels.

In comparison with reefs in most of the other sections of the GBR, John Brewer is relatively isolated from neighboring

reefs (see Figure 1). However, its location on the inner edge of the reef matrix means that direct wave energy from seaward of the GBR is greatly attenuated and transformed before reaching John Brewer. The nearest reef in the windward direction (east to southeast) is Lodestone Reef, which is roughly one fifth the size of John Brewer and approximately 7 km to the southeast (Figure 1).

The primary criterion in the selection of the location of the experiment on the reef was the need for a simple geometry so that the physics of the problem could be more easily understood and also so that results from this experiment could be more easily generalized for other sites. The location of the experiment is indicated on Figure 2. The false front dips to below 20 m LAT almost 1 km northeast of the chosen location, and the reef front is straight and reasonably free from indentations or protuberances for about 100 m on either side of the main measurement location.

Figure 2 shows the relative positions of the wave-measuring instruments. A Waverider buoy (W1) was located approximately 500 m seaward of the reef front in a depth of approximately 50 m. The predominant direction of the waves is from the east-southeasterly direction rather than the south-southeasterly direction of the normal to the reef front at the reef flat experimental site. Therefore W1 was not positioned on a line normal to the reef front, but was located approximately 500 m to the northeast.

On the reef flat (depths less than 3 m), wave and water level measurements were made using surface piecing transmission line staffs called "Zwarts" poles [Zwarts, 1974]. Data from the wave staffs were logged on site. Figure 3 is a cross-sectional view of the reef front and reef flat and shows the position of the wave staffs in more detail. The four wave staffs were aligned along a linear array normal to the reef front. The most seaward staff, S1, was located 27 m from the reef front and staffs S2, S3, and S4 were located at intervals of 42, 49, and 50 m, respectively, moving away from reef edge and toward the lagoon.

No directional wave data were obtained during the field experiment. However, visual observations during more than 40 days spent at the experimental site indicated a pattern of wave direction during all but very weak wind conditions such that (1) the mean wave direction seaward of the reef was always very closely aligned with the local wind direction, and (2) on the reef flat the wave crests during mid tidal and low tidal levels were aligned parallel to the reef front. This second point was observed not only at the experimental location, but also at other locations along the windward edge of John Brewer Reef. This refraction is greater than that predicted from the application of Snell's law. Such an analysis, using the mean water level during measurements of $h = 1.5$ m and most common peak wave period of 5 s, gives reef flat angles of 19° and 14° (reef normal is 0°) for incident wave angles (at W1) of 45° and 30° , respectively. Visual observations indicated and aerial photos confirm that reef flat wave directions were significantly more reef-normal than indicated by these calculations.

The primary data collection effort was over a 6 week period from September 1 to October 15, 1988. For the first few days, data were recorded at hourly intervals for all instruments. After 6 September, data for the wave staffs were recorded at 2 hour intervals. The record at all six wave measuring instruments is almost complete for a 20-day period (September 2 to 22), during which a wide range of conditions was recorded.

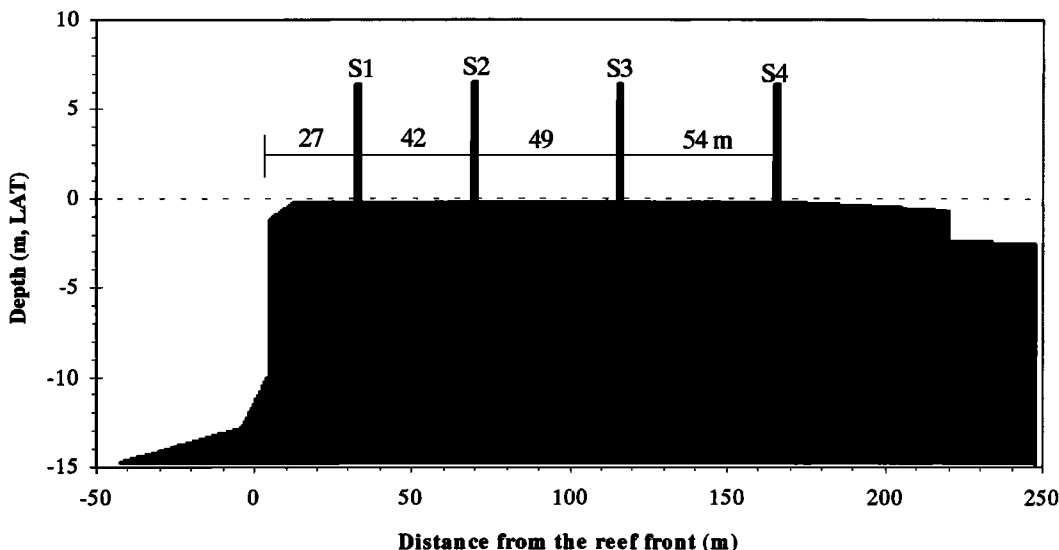


Figure 3. Cross section at reef front along the line of the wave staff array.

A time series containing 2048 samples of water level at a discrete time interval of $\Delta t = 0.3906$ s for a total time series length of 13.3 min (800 s) was recorded at each data collection time from the Waverider buoy. For the wave poles, a 20-min (1200 s) time series of water level with 4800 samples at $\Delta t = 0.25$ s was recorded at each data collection time.

More than 3000 individual time series were gathered. There were 286 times when all six instruments were operating, and of these, 259 were times when waves were approaching from the northeasterly to southerly directions for which the experiment was designed. Data were collected for a wide range of tide and wind conditions. We believe that this data set is the largest and most comprehensive ever collected in this environment.

4. Wave Data Summary

The variance spectral density $S(f)$ was calculated for each of the time series using a fast Fourier transform. For the Waverider the raw spectral ordinates were smoothed in the frequency domain by averaging 15 raw ordinates (30 degrees of freedom), which resulted in a smoothed spectral frequency resolution of 0.0188 Hz. For the wave staffs the raw spectral ordinates were smoothed in the frequency domain by averaging 20 raw ordinates (40 degrees of freedom), which resulted in a smoothed spectral frequency resolution width of 0.0195 Hz. An example spectrum at a wave pole location is shown in Figure 4, which includes the 90% confidence bands on selected spectral ordinates.

Several wave height and wave period parameters (from both time and frequency domain analyses) were calculated during the analyses of the data [Hardy, 1993]. Two spectral parameters, the significant wave height H_s and the peak wave period T_p , will be used in analyses presented in this paper. The energy-based significant wave height, defined as

$$H_s = 4\sqrt{m_0} \tag{1}$$

was calculated from each spectrum, where m_0 is the zeroth spectral moment. In this paper the symbol H with the sub-

scripts W1, S1, S2, S3, and S4 will indicate the significant wave height at the subscript location. The 90% confidence interval about the significant wave height was estimated using the method of Donelan and Pierson [1983]. For Figure 4, $H_s = 0.69$ m and upper and lower 90% confidence limits are $H_s = 0.72$ and $H_s = 0.67$ m, respectively. This confidence interval fell in a very tight range averaging approximately $\pm 5\%$ for the data set.

In tests of several methods for the calculation of the peak spectral period, Mansard and Funke [1991] recommend

$$T_p = \frac{\int S^5(f)df}{\int fS^5(f)df} \tag{2}$$

This parameter estimates the peak of the spectrum through a weighted average, which helps to reduce the unstable nature of the determination of peak period, especially in broader or multiply peaked spectra.

Figure 5 contains plots of the time series of wind, water level, and wave height parameters for the main experimental

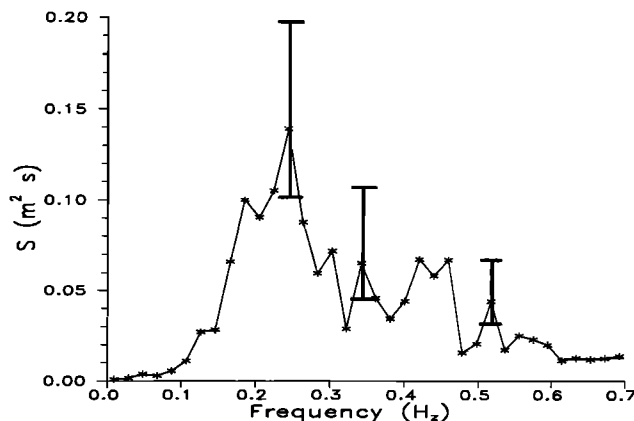


Figure 4. The 90% confidence bands on a reef flat spectrum.

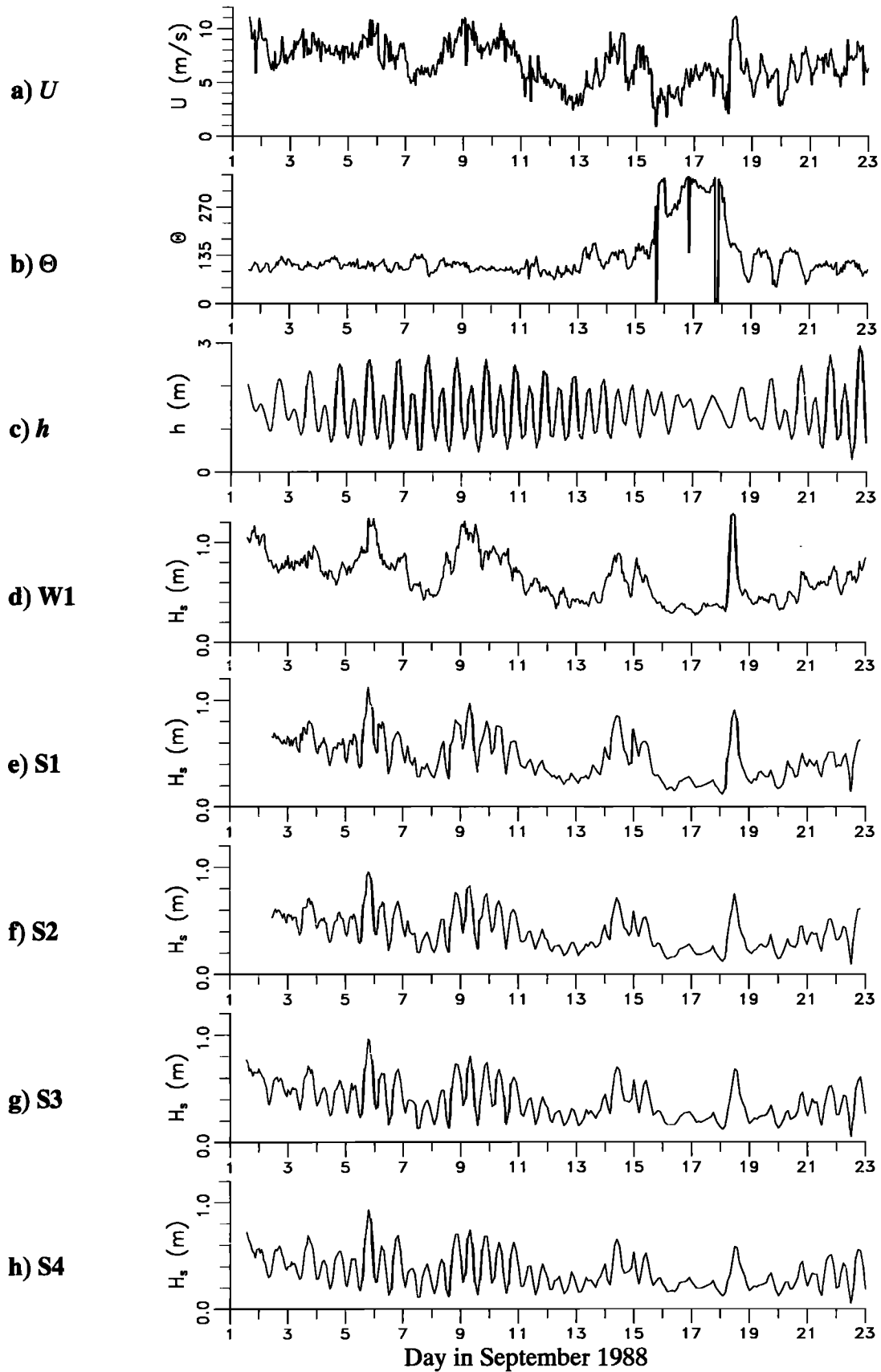


Figure 5. Data set for September 1-22, 1988 showing (a) wind speed, (b) wind direction, (c) water level, and significant wave height at Waverider buoy (d), and four wave staffs (e) S1, (f) S2, (g) S3, and (h) S4.

period, September 1-22, 1988. This period covers a wide range of conditions and contains all the data analyzed in this paper. Figure 5 contains the whole time series for this period for the following eight parameters: Figures 5a and 5b are plots of wind speed U and direction θ (measured at Myrmidon Reef, see Figure 1); Figure 5c is a graph of water level h relative to the reef flat; and finally, Figures 5d to 5h are plots of significant wave height at W1, S1, S2, S3, and S4.

The wind speed U was between 5 and 10 m s^{-1} for most of the period, as is seen in Figure 5a. Figure 5b shows that wind direction was almost continuously between east and southeast, except for a 2 day period centered on September 16.

As seen in Figure 5c, the experiment covered a time period just longer than one spring-neap tidal cycle. The water depth h over the reef flat varied from 0.24 m to 2.97 m, and the average level (at which data were collected on the reef flat) was $h = 1.46$ m. The water depth was remarkably constant among the wave staff locations. The variation, among locations, in average water levels recorded during a 20-minute wave record was very rarely more than 10 mm. Wave-induced water level changes appear to elevate the water level almost horizontally across the reef flat (at least in that region between S1 and S4).

The significant wave height H at W1 (Figure 5d) varied from 0.2 m to 1.3 m. The peak period, T_p , not plotted in Figure 5, varied between 2.1 s to 9.5 s. The time history of significant wave height at W1 (Figure 5d) has an obvious, visual, positive correlation with wind speed (Figure 5a). A cross-correlation analysis, in which the wind speed time history was lagged relative to the wave height time series at W1, gives a cross correlation coefficient of $r = 0.8$ at lags of -1 and -2 hours. This indicates a rapid response in wave energy to changes in wind speed and indicates the waves measured at W1 are dominated by sea rather than swell.

The significant wave heights at the reef flat stations (Figures 5e to 5h) show a positive correlation with H_{W1} . However the time histories of significant wave height at these leeward stations have a strong tidal modulation. As expected, the wave heights on the reef flat are reduced appreciably during lower tide levels. A trend showing the reduction in wave energy from W1 through the reef flat stations (S1, S2, S3, and S4) is significant at all tide levels. As an example, note the spike of high winds on the morning of September 18 that causes a spike in wave height that is noticeably attenuated along the instrument array.

In contrast to the dependence of reef flat wave heights on water depth, the significant wave height at W1 is very poorly correlated with water level. The correlation coefficients at all lags were close to zero. Although the field experiment did not collect wave data seaward of the GBR, there is little doubt that much of the energy generated seaward of the GBR is attenuated before reaching John Brewer Reef. The measurements of Wolanski [1985] indicate much more energy seaward of the GBR ($H_s \approx 4$ m) than was measured for comparable meteorological conditions. The arrival of "outside" wave energy at W1, after attenuation over upwind reefs during low tide, would be expected to be spread over a considerable time span due to the scattered nature of the reef matrix. Thus it is not surprising that the wave time series at W1 shows no correlation with the local tidal level.

The main data set summarized in Figure 5 was sorted to exclude wind conditions outside of the band of directions (between 45° and 225°) for which waves would approach the study site from deep water. Also, data were excluded if not simultaneously recorded at each of W1, S1, S2, S3, and S4. The result is 259 times (or $5 \times 259 = 1295$ wave time series) when the winds were blowing from the desired directions and each of these five instruments was recording. These data constitute the primary data set used in the analyses discussed in this paper.

5. Wave Spectra

It is possible to show only a very small proportion of the several thousand wave spectra. Representative spectra are presented in the following sections so that a range of spectral characteristics can be demonstrated.

5.1. Spectra at W1

A wide variety of spectral shapes is observed in the W1 spectra. Often, spectra exhibited multiple peaks, especially during times of lower than average wind energy, when winds show less spatial and temporal consistency. Thus waves from several sources will arrive at W1. At these times of weaker winds, wave energy from these different sources might make a significant contribution to the spectrum. A spectrum that is representative of irregular, multiply peaked spectra is shown in Figure 6. Peaks are often found at or near 0.1, 0.25, and 0.3 Hz. However, the location and magnitude of the peaks show considerable variability. These spectra are best characterized as broad.

Evidence exists in the wave spectra at W1 that some energy from seaward of the GBR does penetrate to John Brewer Reef. Wolanski [1986] reported that the prevailing wave period for a measurement position seaward of the GBR was approximately $T = 10$ s ($f = 0.1$ Hz). Energy at or near this frequency commonly occurs in the spectra from W1 (see Figure 6). During times of higher energy it almost never contributes anything but a small percentage of the total energy and is rarely the peak frequency. At times of lower wave energy this swell energy can become more dominant and is sometimes the peak of the spectrum.

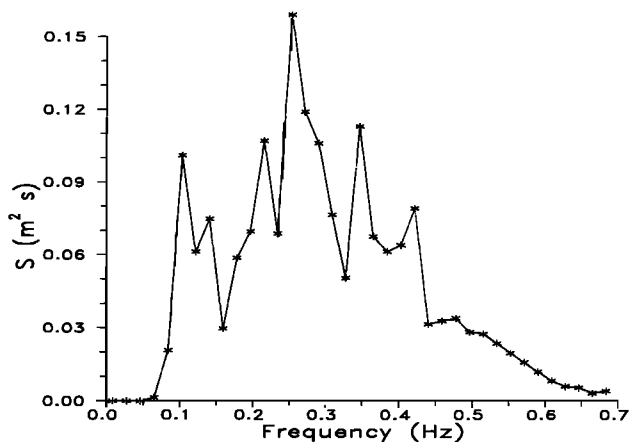


Figure 6. Example of multiply peaked spectrum at W1.

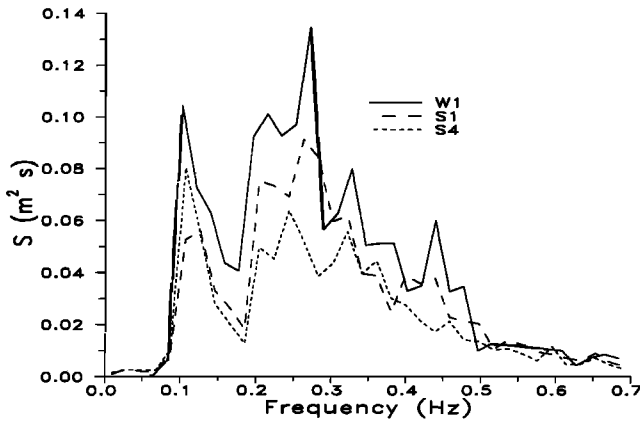


Figure 7. Measured spectral transformation at high tide with $h = 2.48$ m, $H_{W1} = 0.67$ m, $H_{S1} = 0.60$ m, and $H_{S4} = 0.53$ m, where h is water depth and H is significant wave height, with subscripts denoting location.

5.2. Reef Flat Spectra

After the transition from W1 to the reef flat, both the shape and energy level of the reef flat spectra depend strongly on the depth of water over the reef flat. For higher tide levels the changes are smaller as is shown in Figure 7 ($h = 2.48$ m, $H_{W1} = 0.67$ m). At these ratios of incident wave height to water level, the spectra on the reef flat closely mimic the corresponding spectra at W1. The attenuation is greater at the portions of the spectra with higher energy and lower frequency and causes the reef flat spectra to be broader than those at W1.

At lower water levels, transfer of energy from the peak frequency to harmonics of the peak frequency is expected. Figure 8 ($h = 1.48$ m and $H_{W1} = 0.98$ m) clearly shows this. At this time several hours of strong winds followed a prolonged calm period. One of the authors was on the reef flat that morning attempting (unsuccessfully in the rough conditions) to mount a current meter. The waves had a pronounced nonlinear shape: sharp peaks and long flat troughs. There was an obvious principal wave period unlike many times on the reef flat when it was more difficult to visually determine the dominant period. Therefore it is not surprising to see the spectra characterized by a single peak. Spilling breakers began just before S1, and wave breaking continued past S2. Only low-

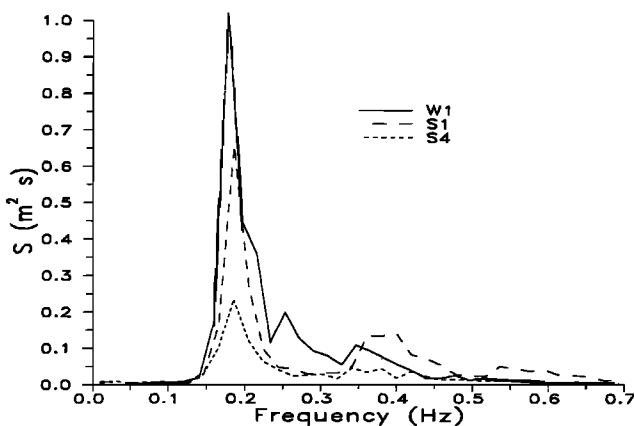


Figure 8. Measured spectral transformation at mean tide with $h = 1.48$ m, $H_{W1} = 0.98$ m, $H_{S1} = 0.91$ m, and $H_{S4} = 0.58$ m.

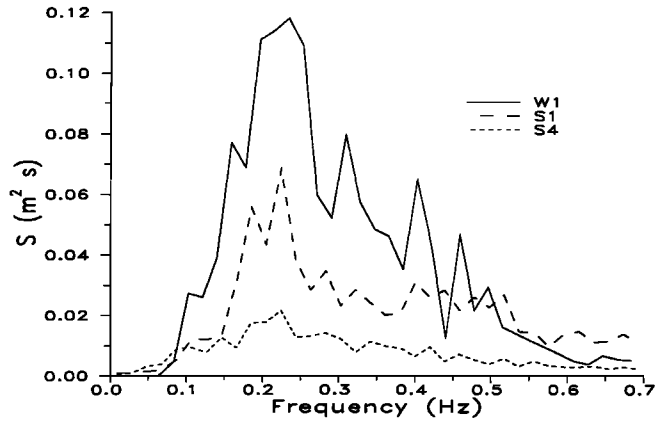


Figure 9. Measured spectral transformation at low tide with $h = 0.98$ m, $H_{W1} = 0.64$ m, $H_{S1} = 0.51$ m, and $H_{S4} = 0.31$ m.

intensity breaking of the largest waves continued after S3. The nonlinearity is indicated in the energy that appears in the spectrum at the first harmonic (≈ 0.38 Hz) of the peak frequency. The spectral ordinates at this harmonic diminish as the waves move from S1 to S4. The energy attenuation is pronounced at the peak of the spectrum. This, in turn, reduces the nonlinearity of the waves and contributes to the reduction of energy at the first harmonic.

The water level at low tide is commonly below 1 m LAT. The attenuation at this depth is shown in Figure 9 in which spectra at W1, S1, and S4 are plotted. The losses between W1 and S1 are approximately the same as those between S1 and S4.

Water levels below 0.5 m occur only during spring tides. As expected, energy attenuation is severe at these low water levels. Figure 10 contains plots of the measured spectra at W1, S1, S2, S3, and S4 for $h = 0.45$ m. The energy loss is so large that the spectrum at the later location cannot even be seen at a linear scale appropriate for the spectrum at W1. At this very low water level, almost all the energy is lost in the vicinity of S1. The spectra at the reef flat stations lose the main peak and become very flat. Note the energy at low frequencies which results from nonlinear wave-wave interactions and from wave-induced changes in the water level. This low frequency energy is found in many of the spectra on the reef

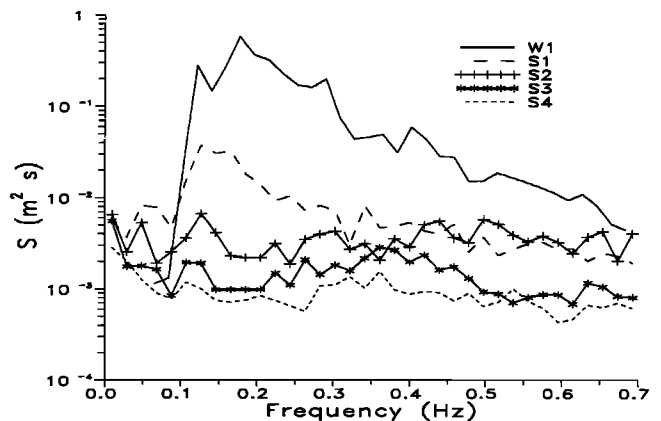


Figure 10. Measured spectral transformation at very low tide with $h = 0.45$ m, $H_{W1} = 0.99$ m, $H_{S1} = 0.32$ m, $H_{S2} = 0.23$ m, $H_{S3} = 0.15$ m, and $H_{S4} = 0.13$ m.

flat, but it is only a significant portion of the total energy if a large amount of dissipation has occurred and the total energy remaining is very small.

6. Spectral Parameters

6.1. Wave Period

As was seen in the preceding section, wave spectra measured during the field experiment are often irregular, and energy is spread over a wide range of frequencies. Therefore characterizing a spectrum with a single wave period is often less than satisfactory. Nevertheless, some insight can be gained by examining the peak period.

The relationship between wave periods at W1 and on the reef flat is shown in Figure 11, which is a scatterplot of T_p at S1 versus T_p at W1. For wave periods below 5 s there is a close correspondence between the reef flat and offshore values. At wave periods above 5 s there is a good deal of scatter in the data. These longer wave period data are often low energy episodes with a significant swell component (especially if $T_p > 6$ s). The transformation and attenuation across the reef front will vary, depending on the relative directions of the sea and swell components. The reef flat wave periods should be slightly shorter than the incident wave periods, since breaking and bottom friction over the reef flat will remove more energy at longer wave periods, thus shifting T_p to shorter values. This is supported by the data shown in Figure 11.

Scatterplots of the relationship between H_s and T_p for W1 and S4 (Figure 12) show some interesting characteristics. There is a well-defined envelope for wave periods less than 5 s, under which the value of H_s is limited at a given value of T_p . The level of the envelope reduces from W1 (Figure 12a) to S4 (Figure 12b), as would be expected due to, first refraction and, then, energy attenuation in shallow water. At first, it might seem that the envelope is a wave steepness limitation. However, defining wave steepness as H_s/L_p , where L_p is a wavelength corresponding to T_p , the steepnesses along the envelope are about 4%, which is significantly less than that which would indicate wave breaking (e.g., $\approx 12\%$ [Chen and Wang, 1983]). Instead, the envelope appears to be related to the upper range of significant wave heights that are predicted by fetch-limited wave generation equations.

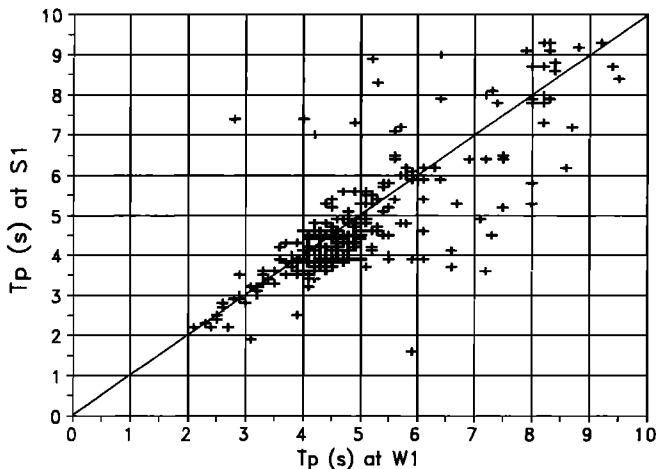
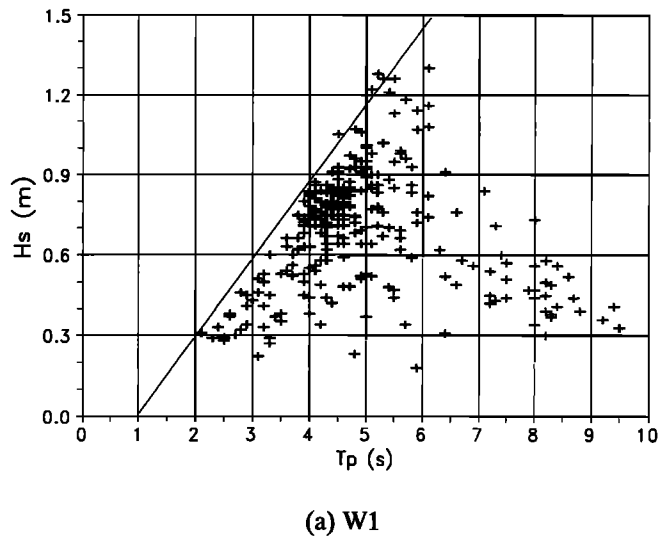
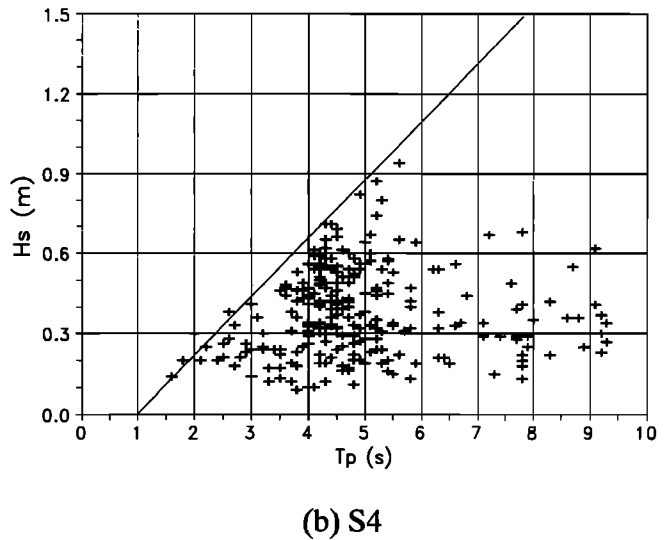


Figure 11. Scatterplot comparing peak spectral period T_p at W1 and S1.



(a) W1



(b) S4

Figure 12. Scatterplots of H_s versus T_p at (a) W1 and (b) S4.

Young [1992] reformulates, in terms of significant wave height and spectral peak period, the fetch-limited spectral equations of Donelan *et al.* [1985]. For a wind speed representative of the field experiment ($U = 10 \text{ m s}^{-1}$) the values of H_s from Young [1992] correspond well (they are slightly larger) with values along the top of the envelope in Figure 12a. For example if $T_p = 4$ s then Figure 12a gives $H_s = 0.89$ m and Young [1992] gives $H_s = 1.0$ m. The field data should show slightly less energy since the fetch upwind of John Brewer Reef does have obstructions (upwind reefs), which would truncate the energy available, especially at lower frequencies.

At wave periods above approximately 6 s, the envelope in Figure 12 is not defined, since significant wave heights above 1.2 and 1.0 m were rare at W1 and the wave staffs, respectively. This indicates that either fetch or wind duration are limited. Since wind durations are sufficient (Figure 5a), the $T_p \approx 6$ s limit appears to be the fetch limit for wind speeds of approximately 10 m s^{-1} . Wave periods above 6 s indicate times when local waves are small and when low-energy swell, which has penetrated the GBR matrix, is dominant.

6.2. Wave Height

Two factors are important in governing the magnitude of wave energy on the reef flat. These are the magnitude of incident energy, which will be represented here by H_{W1} , and the depth of water over the reef flat h . The combined effect of these two factors on the significant wave height at the reef flat stations can be seen in Figure 13, where significant wave height contours for the four reef flat stations are plotted as a function of H_{W1} and h . A general pattern is evident in Figures 13a – 13d. At the shallowest depths the magnitude of wave energy on the reef flat becomes increasingly insensitive to incident wave energy and is controlled by water depth. As the depth becomes greater, the opposite occurs, with the incident wave energy becoming the dominant factor.

Figure 13a, the plot for S1, most clearly shows this dichotomy. If a line were drawn from the origin to separate the two regions, the slope of the dividing line would be in the range $0.8 < H_{W1}/h < 0.4$. To the left of this line, depth dominates; to the right, incident energy is most important. Since S1 is positioned close to the reef front and therefore the breaking point, the intersection between these two regions is indicative of the threshold of the main shallow water dissipation mechanism,

wave breaking. For the deep water region, little or no wave breaking occurs, whereas for the shallow water region, wave breaking causes a depth limitation on wave energy. The separation between breaking and nonbreaking will be also discussed in the next section.

Plots of the contours of significant wave height at the remaining stations (S2, S3, and S4) are shown in Figures 13b to 13d. These plots show that wave energy is no longer independent of depth for larger values of h . As the waves on the reef flat move past S1, energy loss from bottom friction on the rough coral surface becomes increasingly important. Hardy [1993] suggests a bottom friction coefficient for use on coral reef flats that is approximately 1 order of magnitude higher than that normally used for sandy bottoms. Therefore significant energy losses due to bottom friction are expected to occur over the relatively short distances between the reef flat stations (≈ 50 m). For larger values of h this effect causes the slope of the contours, which are almost horizontal in Figure 13a, to become increasingly negative from Figures 13b to 13d.

Figure 14 contains plots of significant wave height versus water depth over the reef flat for W1, S1, S2, and S4. The plot for W1 (Figure 14a) shows no indication of a dependence of wave height on water level. In contrast to Figure 14a, Figures

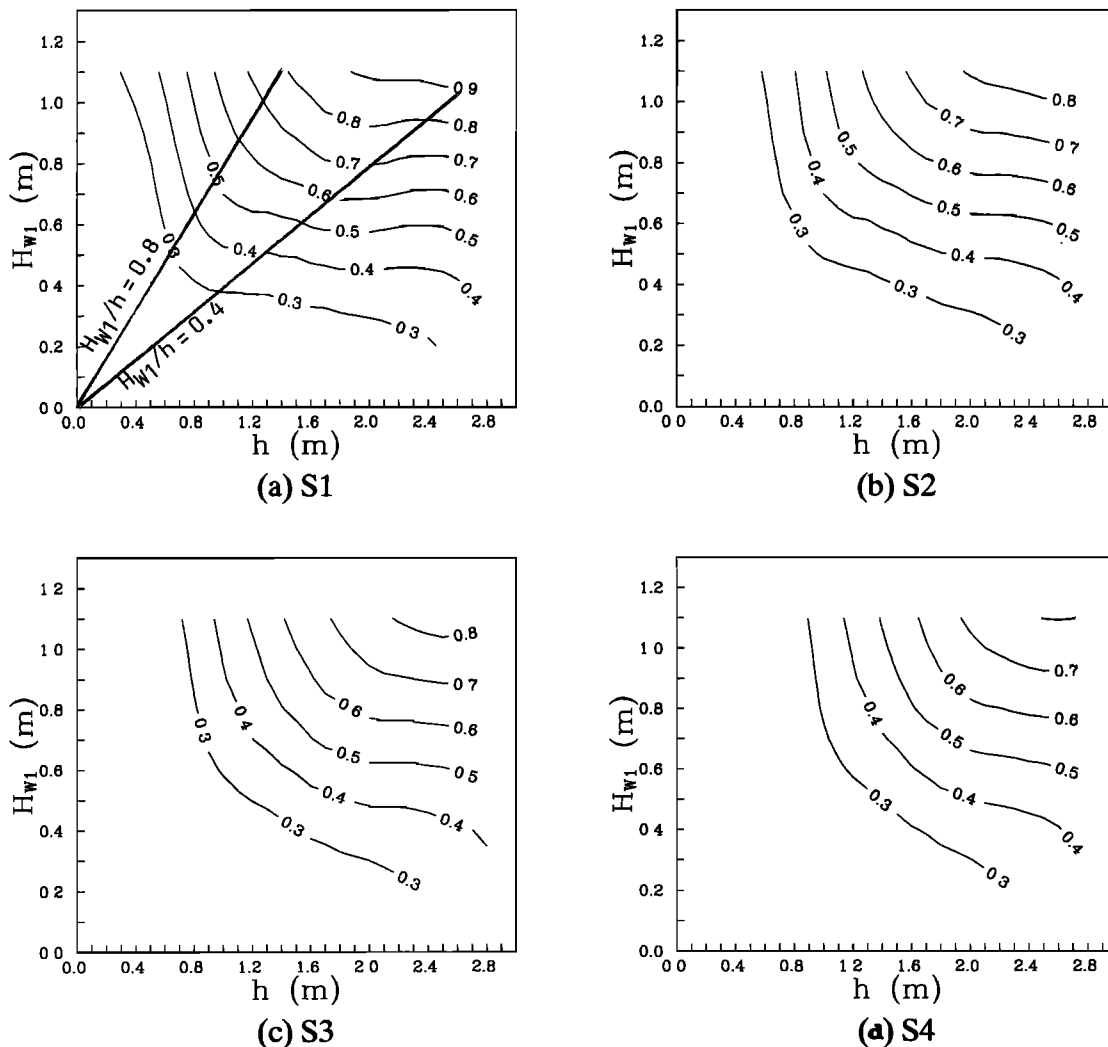


Figure 13. Contours of significant wave height at reef flat stations as a function of incident wave height H_{W1} and water depth over reef flat h at (a) S1, (b) S2, (c) S3, and (d) S4.

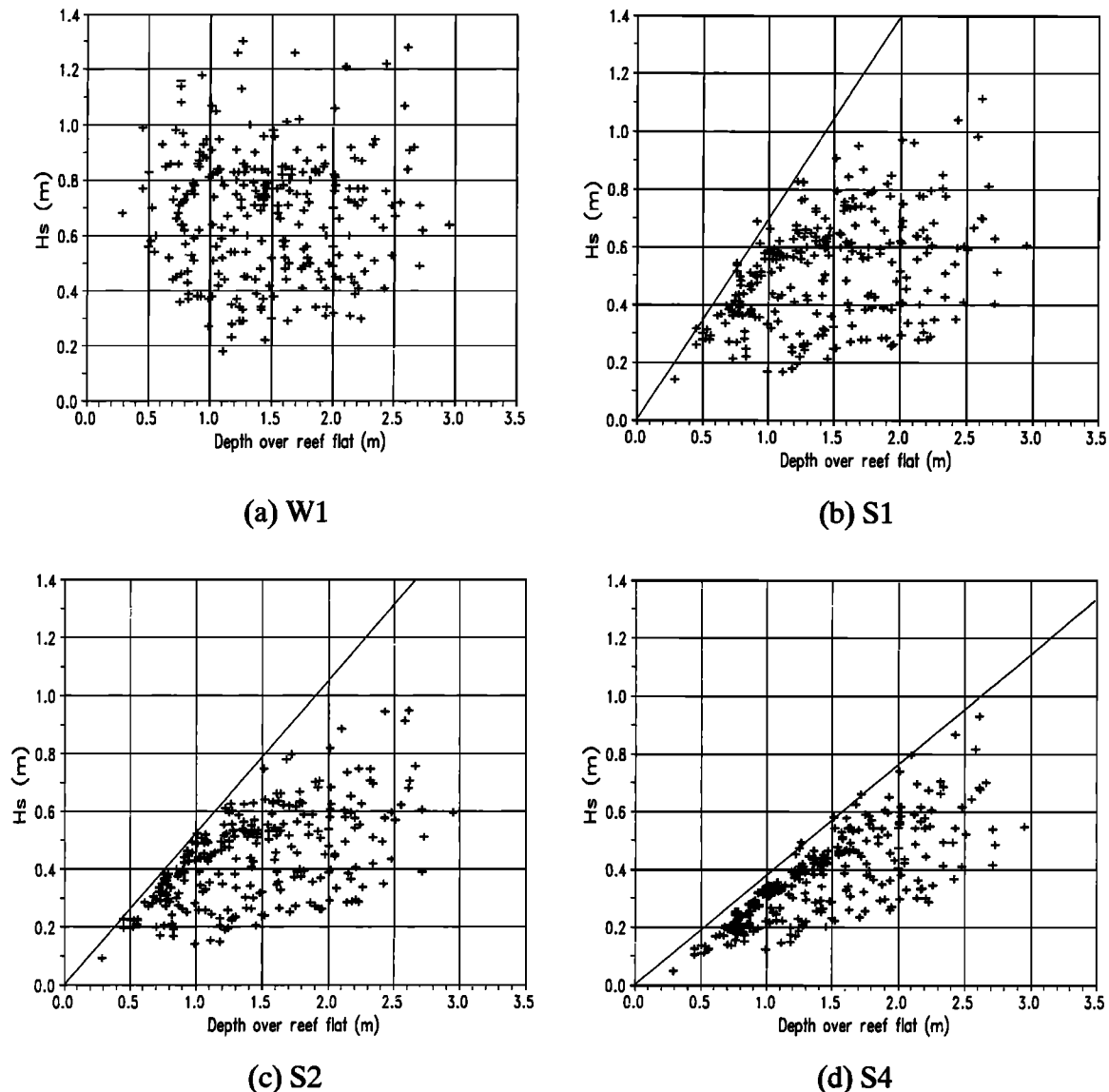


Figure 14. Scatterplots of significant wave height versus water depth over reef flat at (a) W1, (b) S1, (c) S2, and (d) S4. Lines are drawn for recommended upper envelope.

14b to 14d all show a marked dependence of H_s on tide level for the reef flat stations.

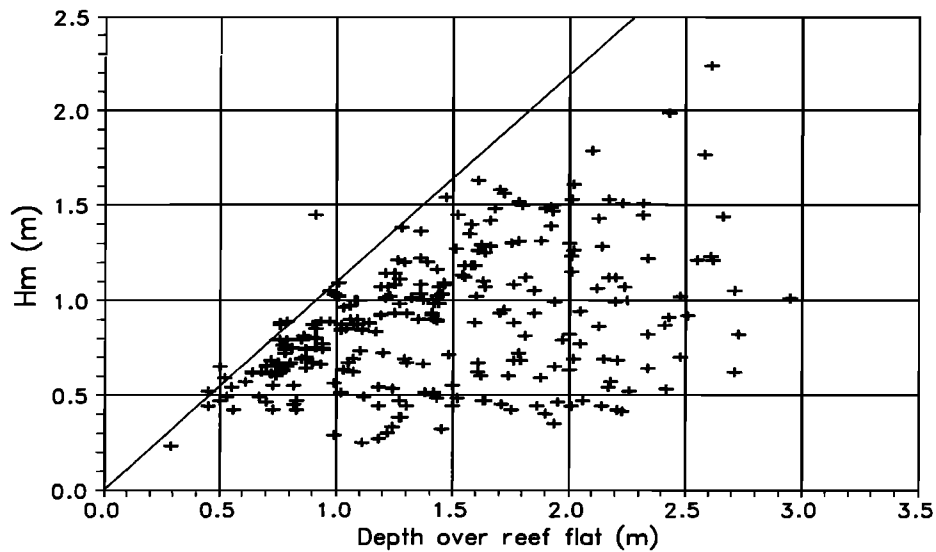
The envelope in Figures 14b to 14d is well defined and reasonably linear, especially at lower water levels. Using the relationship $H_s = \gamma h$, where γ is the slope of the upper envelope of the H_s versus h relationship, γ reduces from approximately 0.70 at S1 to approximately 0.38 at S4. These results are similar to results from monochromatic laboratory experiments conducted by *Horikawa and Kuo* [1967], in which waves broke on the seaward edge of a horizontal shelf, fronted by a sloping offshore bottom. Values of γ from their experiment decreased from 0.80 at the shelf edge (recall that S1 was 27 m from the reef edge) to 0.35 to 0.43 across the shelf.

A zero-downcrossing time domain analysis was conducted, and the maximum wave height H_m of each time series was calculated. Plots of H_m versus h for S1 and S4 are presented in Figure 15. As expected, the dependence on depth is clear for the four wave staffs.

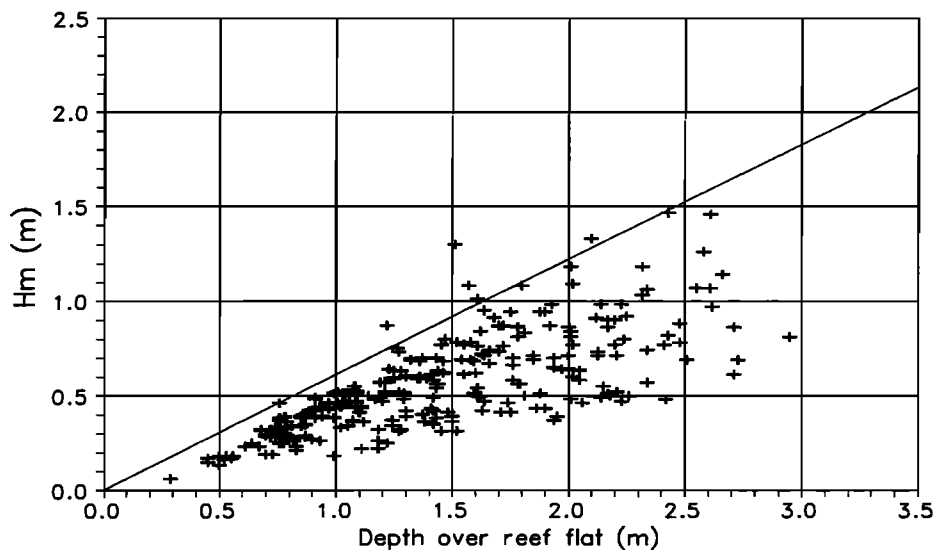
The envelope of the ratio of maximum wave height to water depth γ_m fell from approximately 1.1 at S1 to 0.6 at S4. Laboratory data for the maximum height of regular waves on horizontal or very flat bottoms, i.e., conditions similar to reef tops, give a maximum value of $\gamma_m = 0.55$ [*Nelson, 1985; Nelson and Gonslaves, 1992*].

7. Wave Breaking

As was shown in Figure 10, the main effects on a spectrum after wave breaking are a marked reduction in total wave energy, with most of the energy loss occurring in the region near the peak. This broadening of the spectrum on the reef flat may not be solely due to shifts of energy to bound harmonics such as shown in Figure 8. Free waves can be induced during both wave breaking and in the transition over the step-like geometry. *Byrne* [1969] shows evidence of higher harmonics created in nonbreaking waves that crossed the continental shelf. *Battjes and Beji* [1991] give experimental evidence of induced



(a) S1



(b) S4

Figure 15. Scatterplots of maximum wave height versus water depth over reef flat at (a) S1 and S4. Lines are drawn for recommended upper envelope.

waves and significantly broadened spectra for waves traveling across a shallow shoal. In their experiment it is significant that only longer waves showed evidence of induced free waves. No induced free waves were apparent in the time histories of shorter waves, although they did exhibit nonlinear wave shape over the shoal.

For John Brewer Reef, waves are wind sea rather than swell. They are relatively short (compared to the swell in Hawaii, for example). Also, the incident spectra tend to be relatively broad rather than narrow banded. Therefore the energy of induced free waves is expected to be small, and the detection of any free wave energy that is shifted to higher harmonics will be difficult. Either a bispectral analysis [Hasselmann *et al.*, 1962] or a tuned array of instruments [e.g., Donelan *et al.*, 1985] would be necessary to detect and separate bound and free energy in the harmonics of the spec-

trum. Data collection for such analyses was not conducted for the John Brewer Reef experiment.

7.1. Initiation of Wave Breaking

As was discussed in the introduction, a wave model of the GBR region will primarily be a wave generation model operating in the frequency domain, especially in the regions before and after the windward reef edge. Therefore remaining in frequency domain for the modeling of dissipation over a coral reef flat offers a more direct technique rather than switching to time domain (wave-by-wave approach) for the reef flat and then returning to frequency domain for modeling leeward regions. Hardy [1993] used the ratio of significant wave height to water depth at the threshold between breaking and non-breaking λ_{th} as a parameter to initiate breaking dissipation in a reef flat spectral wave model.

In order to investigate incipient breaking conditions, information is needed at the reef front (RF). The significant wave height at the reef front is obtained by transforming spectra measured at W1 to RF by accounting for the effects of directional spreading, shoaling and refraction, as well as the reflection and transmission at the abrupt transition in depth at the reef front.

The directional spreading function proposed by *Donelan et al.* [1985] was used to convert the frequency spectrum measured at W1 to a frequency-directional spectrum. A straight and parallel bathymetry was assumed seaward of the reef front, and Snell's law was used to determine the change in wave angle due to refraction. The reef flat is modeled as an infinite step, and the transmission coefficient K_T , calculated following *Massel* [1983], by matching energy flux and surface elevation at the reef front, is given by

$$K_T = \frac{2}{1 + \frac{c_{gRF} \cos\theta_{RF}}{c_{gW1} \cos\theta_{W1}}} \quad (3)$$

where θ is the angle of wave approach relative to a normal to the reef front, and c_g is the group velocity at the subscript location.

The algorithm for the transformation of the directional spectrum is based on that derived by *Le Méhauté and Wang* [1982], which is

$$S_{RF}(f, \theta_{RF}) df d\theta_{RF} = K_s^2 K_r^2 S_{W1}(f, \theta_{W1}) df d\theta_{W1} \frac{\partial \theta_{W1}}{\partial \theta_{RF}} \\ = \frac{c_{W1} c_{gW1}}{c_{RF} c_{gRF}} S_{W1}(f, \theta_{W1}) df d\theta_{W1} \quad (4)$$

where K_s and K_r are the shoaling and refraction coefficients, c is the wave velocity at the subscript location, and the correspondence between θ_{RF} and θ_{W1} is given by an inverse direction function (in this case Snell's law). Equation (4) is adapted for the case of transmission over an infinite step (following *Massel* [1989]) to give

$$S_{RF}(f, \theta_{RF}) df d\theta_{RF} = K_T^2 S_{W1}(f, \theta_{W1}) df d\theta_{W1} \frac{\partial \theta_{W1}}{\partial \theta_{RF}} \quad (5)$$

in which the transmission coefficient replaces the shoaling and refraction coefficients. Evaluation of the Jacobian in eq (5) gives

$$S_{RF}(f, \theta_{RF}) df d\theta_{RF} = K_T^2 \frac{c_{W1} \cos\theta_{RF}}{c_{RF} \cos\theta_{W1}} S_{W1}(f, \theta_{W1}) df d\theta_{W1} \quad (6)$$

which is the governing equation used in the modeling from W1 to RF. *Hardy* [1993] found that inclusion of transmission/reflection (equation (6)) produced only very small differences in reef flat spectra compared with spectra modeled without those effects (equation (4)).

Figure 16 contains plots of H_s/h on the reef flat (S1, S2, S3, and S4 for Figures 16a, 16b, 16c, and 16d, respectively) ver-

sus H_{RF}/h , where H_{RF} indicates the significant wave height at the reef front. In general, the data of the plots in Figure 16 fall into two distinct segments, each of which can be approximated by a straight line. Along the lower limb, which is at smaller values of H_{RF}/h , the data closely follow a one-to-one correspondence between H_s/h and H_{RF}/h . The upper limb rotates in a clockwise direction from S1 to S4, going well past horizontal by S4. In Figures 16c and 16d, bottom friction makes a significant contribution to the orientation of the upper limb, especially at larger values of H_{RF}/h , where the frictional losses will be greater. The location of the intersection between the two segments, as an indication of the initiation of wave breaking, and also the level of the upper limb, as an indication of the energy at the end of breaking, are of interest.

Visual observations during the field experiment indicated that S1 was the wave staff located closest to the breaking point. If breaking did not occur, then one would expect that the values of H_s/h at RF and S1 would be approximately equal. This is the case for values of H_s/h below about 0.5 in Figure 16a. In this lower segment of the graph, values of H_s/h tend to be slightly larger at RF than at S1. This is as it should be, since some bottom frictional dissipation is contained in the results measured at S1.

In Figure 16a, above approximately $H_{RF}/h = 0.5$, a greater loss in energy is indicated. It is clear that above $H_{RF}/h = 0.6$, the values of H_{S1}/h are well below values of H_{RF}/h . Figures 16b to 16d, for S2 to S4, show more clearly the joint of the two segments. There is a progressive downward trend in all the values of H_s/h at the wave staffs compared with the values at RF as the waves cross the reef flat. This trend is pronounced in the upper limb but it is also noticeable, although much smaller, in the lower limb. The value of the ordinate at the intersection between the upper and lower limbs does not remain at the same level, but gradually decreases from S1 to S4.

The evidence in Figure 16 indicates that the threshold between breaking and nonbreaking conditions is somewhere in the range $0.4 < \gamma_{th} < 0.6$ at the reef front. As wave energy increases for a given water depth so that H_{RF}/h becomes approximately 0.40, wave breaking will occur for only the very largest waves in a times series. Then as the value of H_{RF}/h continues to increase, a larger percentage of the waves will break. Identifying the absolute bottom value of H_{RF}/h at which wave breaking occurs is difficult since wave height distributions could vary considerably for a fixed value of significant wave height. At S1 the average value of the ratio of maximum to significant wave height was $H_m/H_s = 1.7$ and the greatest ratio was $H_m/H_s = 2.3$. Very few data collection times had ratios greater than $H_m/H_s = 2.0$.

Using the identity

$$\frac{H_m/h}{H_m/H_s} = \frac{H_s}{h} \quad (7)$$

and adopting a monochromatic breaking criteria, $H/h \approx 0.8$ ($H/h = 0.78$, [*McCowan*, 1894]; $H/h = 0.83$, [*Williams*, 1981; *J. Fenton*, personal communication, 1993]) by applying it to the maximum wave height, indicates that the maximum wave would begin breaking at values of H_{RF}/h of approximately 0.4 and 0.45 for values of H_m/H_s of 2.0 and 1.7, respectively. These calculations indicate that for values of H_{RF}/h greater

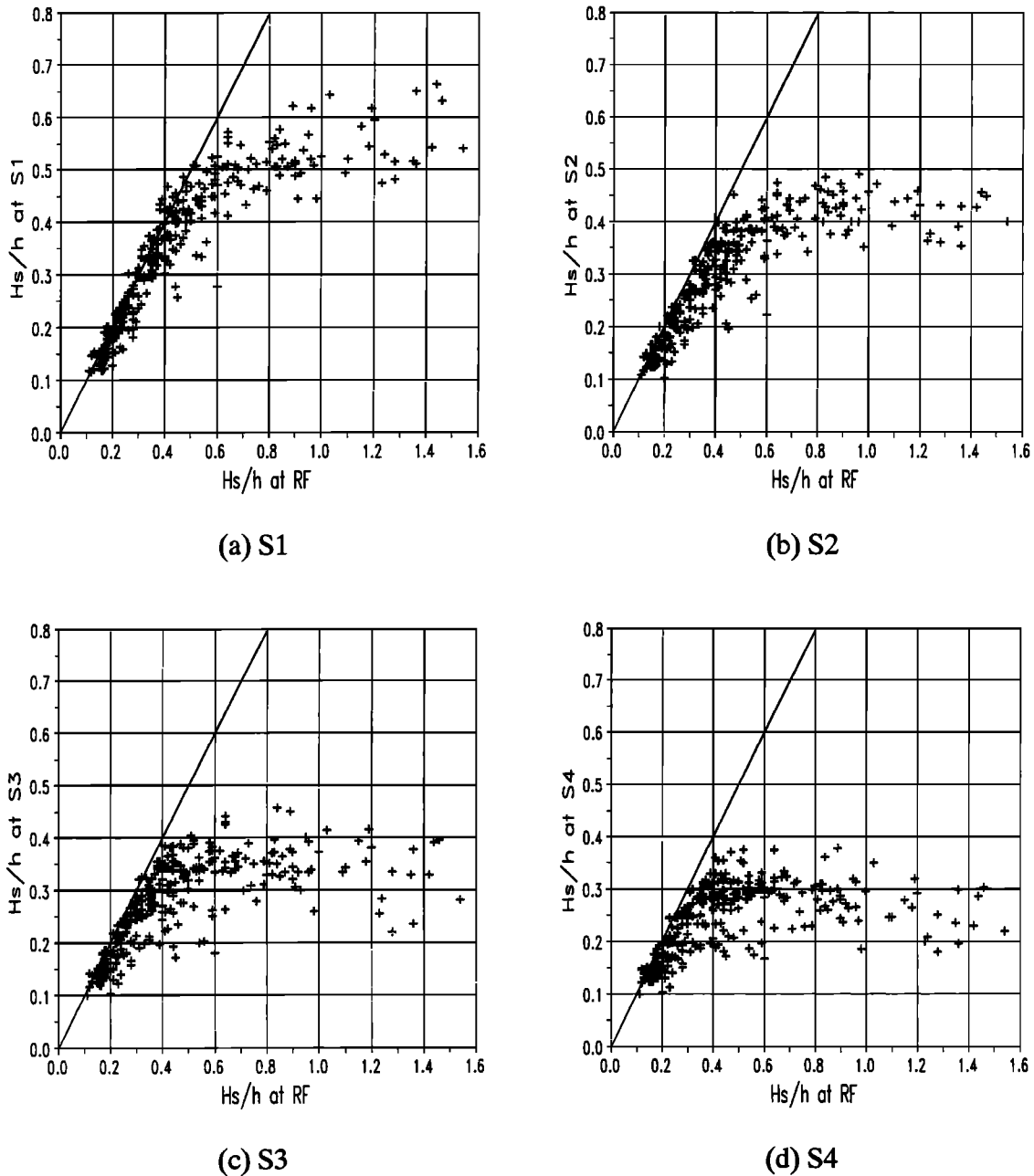


Figure 16. Scatterplots of H_{RF}/h (where RF is reef front) versus H_s/h at wave staffs (a) S1, (b) S2, (c) S3, and (d) S4. Reference lines drawn at a 1:1 correspondence.

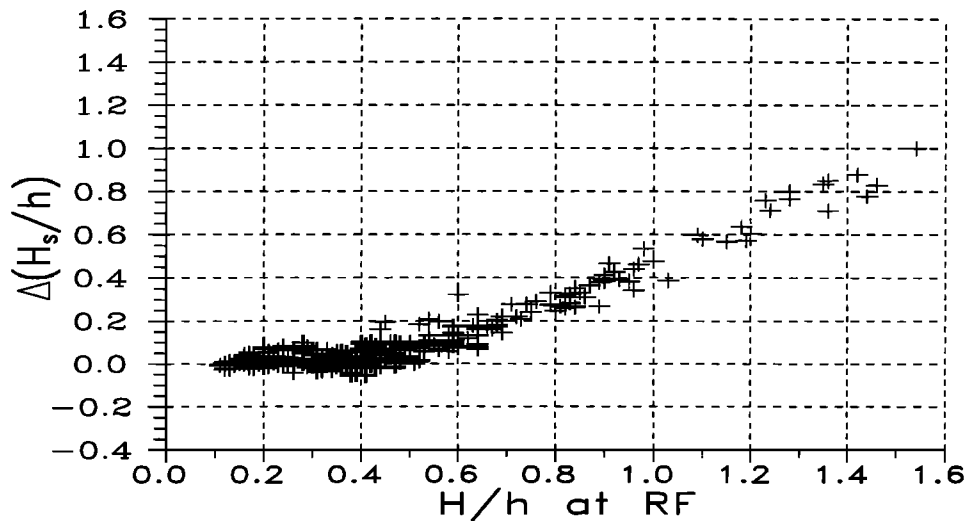
than about 0.40 some dissipation due to breaking may be present. This conforms well with the evidence in Figure 16.

Another way to view the data of Figure 16 is shown in Figure 17 which shows $\Delta H/h$ versus H_{RF}/h . In these plots, $\Delta H/h$ is the difference between the ratio of wave height to water depth at the reef front and at the wave staffs. Figures 17a and 17b are for S1 and S4, respectively. In essence, these plots give an indication of the magnitude of energy losses from the reef front to the wave staffs caused by the combined effects of bottom friction and wave breaking. As in Figure 16, the plots in Figure 17 have a distinct pattern that separates into two linear trends. In Figure 17a, for values of $H_{RF}/h < 0.5$, the trend is roughly horizontal, which indicates that losses are not a function of H_{RF}/h . Breaking is nonexistent or very minor for

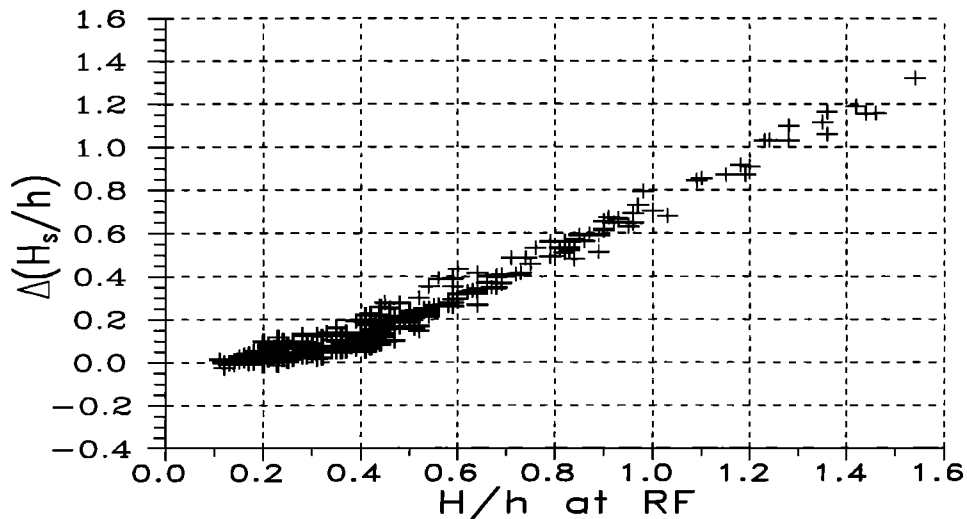
these data, so the data scatter occurs about a horizontal line. For $H_{RF}/h > 0.5$ the trend has a positive slope, which indicates greater losses with increasing values of H_{RF}/h . Wave breaking is an important component of the total losses for these data, and the losses due to breaking will increase with H_{RF}/h .

Notice that in moving from Figure 17a to 17b, the lower limb of these plots ceases to be horizontal. With increasing distance from RF to the location of measurement, the differences in bottom friction as a function of H_s/h begin to become noticeable, and the slope of the lower limb becomes increasingly positive.

The position of the intersection between the two limbs in Figure 17a (S1) is an indicator of the threshold between breaking and nonbreaking. The data scatter evident in the plot



(a) S1



(b) S4

Figure 17. Scatterplots of $\Delta(H_s/h)$ versus H_{RF}/h at (a) S1 and (b) S4.

is due to both measurement and modeling error, but it is also due to the inherent lack of a sharply defined breaking threshold. An abrupt transition between breaking and nonbreaking based on the parameter of significant wave height does not exist. The presence or absence of wave breaking would be determined by the distribution of individual wave heights in the time series, and as stated previously, the distribution can vary for a given value of H_s . Unfortunately, the distribution is unknown, and assuming a distribution (e.g., Rayleigh) adds its own uncertainty into the process. Despite these difficulties, Figure 17 indicates a demarcation between greater dissipation of combined breaking and bottom friction compared with that from bottom friction alone. It is seen in Figure 17a that the intersection between the horizontal lower limb and the sloped upper limb occurs at approximately $H_{RF}/h = 0.5$. This value confirms that suggested by Figure 15.

A linear regression analysis was conducted to fit straight lines to both limbs of Figure 17. The goal was to more tightly

define the breaking point. However, the subjective decisions necessary to define the beginning and end points of the limbs did not allow that analysis to be less subjective than a visual inspection of Figure 17. On the basis of the evidence shown in Figures 16 and 17, the authors recommend $\gamma_{th} = 0.50$.

7.2. Cessation of Breaking

Since waves do not lose all of their energy in the surf zone on an offshore coral reef but can continue to propagate after the conclusion of breaking, knowledge of the energy in the wave field at the conclusion of breaking is important for wave prediction in the lee of a coral reef flat. This end of breaking condition γ_E will be estimated from the data as a value of H_s/h (as was γ_{th} in the preceding section).

Monochromatic laboratory results reported by *Nelson and Leslie* [1985] show that nondimensional width of the surf zone, $x/T\sqrt{gh}$ (where x is the distance from the break-

ing point to the cessation of breaking, T is the monochromatic wave period, and g is the acceleration due to gravity), on a coral reef flat is a function of the ratio of wave height to water depth (H/h). Wave conditions with larger ratios required longer nondimensional distances in which to complete the breaking process. A linear relationship was given, but the data presented are for larger nondimensional wave heights than those measured during the field experiment. Monochromatic laboratory data for a coral reef flat [Gourlay, 1994], which correspond to values of H/h presented here, suggest surf zone widths of between 2 and 3 wavelengths ($2 < x/T\sqrt{gh} < 3$).

Unfortunately, the data set, although by far the most comprehensive in a reef environment, has a coarse spatial resolution in the surf zone. Wave breaking cannot be assumed to end at the location of one of the wave staffs. Therefore data that unambiguously indicate the end of breaking do not exist. Visual observations during the field experiment indicated that S2 was the measurement location closest to the point where breaking ceased. This location is 60 m from the beginning of the horizontal reef flat and therefore has a nondimensional distance from the point of breaking in the range $2.6 < x/T\sqrt{gh} < 5.2$ for an assumed average depth of $h = 1.5$ m and peak periods in the range $6 > T_p > 3$ s. Although the correspondence between monochromatic laboratory data and field measurements is uncertain, these calculations indicate that S2 would have been near to the end of breaking for longer wave periods and after the end of breaking for shorter wave periods.

Even though it is recognized that all data at S2 will not be representative of conditions at the cessation of wave breaking, Figure 16b might still provide a reasonable estimate of γ_E . The calculated average value of the ordinate for the upper limb ($0.5 < H_{RF}/h$) is equal to $H_{S2}/h = 0.40$. However, a close inspection of Figure 16b reveals that for $0.5 < H_{RF}/h < 0.6$ there is a wide spread in values of H_{S2}/h ; most are less than 0.4, none is above 0.45, and some are as low as 0.2. It is clear from visual observations, as well as from Gourlay [1994], and Nelson and Lesleighter [1985], that these wave conditions with values of H_{RF}/h just above the threshold of breaking would reach the end of breaking condition well before S2 and would lose additional energy to bottom friction before reaching S2. Thus data more representative of the conclusion of breaking would have a value of H_{S2}/h larger than that calculated by the average of the upper limb of the graph in Figure 16b. Although a precise end of breaking condition cannot be determined directly from the data, based on the evidence in Figure 16b, the value of significant wave height to water depth ratio at the conclusion of breaking has a value in the range $0.40 < \gamma_E < 0.50$.

8. Summary and Conclusions

A field experiment to measure the attenuation and transformation of waves as they cross the windward edge of an offshore coral reef was conducted. The wave spectra are variable in shape at all stations. Indication of swell with relatively low energy is common. The spectra at W1 show evidence of obstructions and energy losses in the fetch, since the significant wave heights calculated are smaller for a given wave period than those predicted by analytical wind sea generation expressions (e.g., Hasselmann *et al.* [1973]). On the reef flat the spectra maintain much of the character of the spectra at W1 during medium and higher tidal levels. At lower water

levels the reef flat spectra flatten and broaden considerably after energy loss due to wave breaking.

On the reef flat the wave energy is controlled by both incident wave energy and the water depth. At higher tide levels, when wave breaking is nonexistent, incident wave conditions are more important. At lower water levels the depth exerts a controlling influence. Depth limited wave energy on the reef flat can be represented by $H_s = \gamma h$ and $H_m = \gamma_m h$, where $\gamma = 0.4$ and $\gamma_m = 0.6$ by S4 (≈ 170 m from the reef front). Much of the energy dissipation appears to occur in the first few wavelengths. For most of the data, wave breaking was largely completed by S2 (69 m from the reef front) and very little dissipation from breaking occurred past S3 (118 m from the reef front). Additional losses would be expected from bottom friction as the waves continue farther across the reef flat on reefs with wider reef flats.

The threshold between breaking and nonbreaking conditions can be satisfactorily characterized by the ratio of significant wave height to reef flat water depth and is given by $H_{RF}/h = \gamma_{th} = 0.5$. The end of breaking is characterized by significant wave height to water depth ratios in the range from $0.40 < \gamma_E < 0.50$.

Acknowledgments. Funding for the field experiment was provided by the (Australian) Marine Science and Technologies Granting Scheme and the Australian Research Council. The assistance of Michael Gourlay of the University of Queensland and Ray Nelson of the University College, University of New South Wales is appreciated. The field experiment would not have succeeded without the considerable experience and effort of Ray McCalister from the Australian Institute of Marine Science. The instrumentation was developed by Darryl Winterbottom and Mary Dalton of University College, University of New South Wales; their skills and professionalism made the project possible. The support of the Australian Cooperative Research Centres Program through the Cooperative Research Centre for the Sustainable Development of the Great Barrier Reef is acknowledged.

References

- Battjes, J. A., and S. Beji, Spectral evolution in waves travelling over a shoal, in *Proceedings of Nonlinear Water Waves Workshop*, edited by D. H. Perigrine, pp. 11-19, Univ. of Bristol, Bristol England, 1991.
- Black, K. P., Wave transformation over a shallow reef, Tech. Rep. 42, 240 pp., Look Lab., Univ. of Hawaii, Honolulu, 1978.
- Byrne, R. J., Field occurrences of induced multiple gravity waves, *J. Geophys. Res.*, **74**, 2590-2596, 1969.
- Chen, Y.-H., and H. Wang, Numerical model for nonstationary shallow water wave spectral transformations, *J. Geophys. Res.*, **88**, 9851-9863, 1983.
- Donelan, M. A., and W. A. Pierson, The sampling variability of estimates of spectra in directional spectra of shoaling gravity waves, *J. Geophys. Res.*, **88**, 4381-4392, 1983.
- Donelan, M. A., J. Hamilton, and W. H. Hui, Directional spectra of wind-generated waves, *Philos. Trans. R. Soc. London A*, **315**, 509-562, 1985.
- Gerritsen, F., Wave attenuation and wave setup on a coastal reef, in *Proceedings of 17th Coastal Engineering Conference*, vol. 1, pp. 444-461, Am. Soc. Civ. Eng., New York, 1981a.
- Gerritsen, F., Wave attenuation and setup on a coastal reef, Tech Rep. 48, 416 pp., Look Lab., Univ. of Hawaii, Honolulu, 1981b.
- Gourlay, M. R., Wave transformation on a coral reef, *Coastal Eng.*, **23**, 17-42, 1994.
- Hardy, T. A., The attenuation and spectral transformation of wind waves on a coral reef, research report, 336 pp., Dep. of Civ. and Syst. Eng., James Cook Univ., Townsville, Queensland, Australia, 1993.
- Hasselmann, K., W. Munk, and G. MacDonald, Bispectra of ocean waves, in *Proceedings of the Symposium on Time Series Analysis*, edited by M. Rosenblatt, pp. 125-139, John Wiley, New York, 1962.

- Hasselmann, K., et al., Measurements of wind-wave growth and swell decay during the Joint North Sea Wave Project (JONSWAP), report, 95 pp., Dtsch. Hydrogr. Inst., Hamburg, Germany, 1973.
- Horikawa, K., and C. T. Kuo, A study of wave transformation inside the surf zone, in *Proceedings of the 10th Coastal Engineering Conference*, vol.1, pp. ASCE, New York, 217-233, 1967.
- Inman, D. L., W. R. Gayman, and D. C. Cox, Littoral sedimentary processes on Kauai, a subtropical high island, *Pac. Sci.*, 17, 106, 1963.
- Jensen, O. J., Waves on coral reefs, in *Proceedings of the 7th Symposium on Coastal and Ocean Management; Coastal Zone '91*, vol. 3, 2669-2680, Am. Soc. Civ. Eng., New York, 1991.
- Kono, T., and S. Tsukayama, Wave transformation on reef and some consideration on its application to field, *Coastal Eng. J.* 23, 45-57, 1980.
- Lee, T. T., and K. P. Black, The energy spectra of surf waves on a coral reef, in *Proceedings of the 16th Coastal Engineering Conference*, vol. 1, pp. 588-608, Am. Soc. Civ. Eng., New York, 1979.
- Le Méhauté, B. and J. D. Wang, Wave spectrum changes on sloped beach, *J. Waterw. Port Coastal Ocean Div. Am. Soc. Civ. Eng.*, 108, 33-47, 1982.
- Lugo-Fernandez, A., Wave height changes and mass transport on Tague reef, a Caribbean reef, north coast of St. Croix, US Virgin Islands, Ph.D. dissertation, 185 pp., La. State Univ., Baton Rouge, La., 1989.
- Mansard, E. P. D., and E. R. Funke, On fitting of JONSWAP spectra to measured sea states, in *Proceedings of the 22nd Coastal Engineering Conference*, vol. 1, pp. 464-477, Am. Soc. Civ. Eng., New York, 1991.
- Massel, S. R., Harmonic generation by waves propagating over a submerged step, *Coastal Eng.*, 7, 357-380, 1983.
- Massel, S. R., *Hydrodynamics of Coastal Zones*, Oceanogr. Ser., 336 pp., Elsevier, Amsterdam, 1989.
- Massel, S. R., Extended refraction-diffraction equation for surface waves, *Coastal Eng.*, 19, 97-126, 1993.
- McCowan, J., On the highest wave of permanent type, *Philos. Mag.*, 38(5), 351-358, 1894.
- Munk, W. H., and M. C. Sargent, Adjustment of Bikini Atoll to ocean waves, *Trans. AGU*, 29, 255, 1948.
- Nelson, R. C., Wave heights in depth limited conditions, *Civ. Eng. Trans.*, 27, pp. 210-215, Inst. Eng. Aust, Canberra, Australia, 1985.
- Nelson, R. C., and J. Gonslaves, Surf zone transformation of wave height to water depth ratios, *Coastal Eng.*, 17, 49-70, 1992.
- Nelson, R. C., and E. J. Lesleighter, Breaker height attenuation over platform coral reefs, in *Proceedings of the 7th Australasian Conference on Coastal and Ocean Engineering*, vol. 2, pp.9-16, Inst. Eng. Aust, Canberra, 1985.
- Roberts, H. H., Physical processes and sediment flux through reef-lagoon systems, in *Proceedings of the 17th Coastal Engineering Conference*, vol. 1, pp. 946-962, Am. Soc. Civ. Eng., New York, 1981.
- Roberts, H. H., S. P. Murray, and J. N. Suhayda, Physical processes in a fringing reef system, *J. Mar. Res.*, vol. 33, 233-260, 1975.
- Roberts, H. H., S. P. Murray, and J. N. Suhayda, Physical processes in a fore-reef shelf environment, In *Proceedings of the Third International Coral Reef Symposium*, pp. 507-515, Uni. of Miami, Miami, Florida, 1977.
- Seelig, W. N., Laboratory study of reef-lagoon system hydraulics, *J. Waterw. Port Coastal Ocean, Div. Am. Soc. Civ. Eng.*, 109, 380-391, 1983.
- Tait, R. J., Wave set-up on coral reefs, *J. Geophys. Res.*, 77, 2207-2211, 1972.
- Williams, J. M., Limiting gravity waves in water of finite depth, *Philos. Trans. R. Soc. London A*, 302, 139-188, 1981.
- Wolanski, E. J., Some properties of waves at the Queensland shelf break, In *Proceedings of the 7th Australasian Conference on Coastal and Ocean Engineering*, vol. 2, pp. 61-70, Inst. Eng. Aust., Canberra, 1985.
- Wolanski, E. J., Observations of wind-driven surface gravity waves offshore from the Great Barrier Reef, *Coral Reefs*, 4, 213-219, 1986.
- Young, I. R., Wave transformation over coral reefs, *J. Geophys. Res.*, 94, 9779-9789, 1989.
- Young, I. R., The determination of spectral parameters from significant wave height and peak period, *Ocean Eng.*, 19, 97-508, 1992.
- Zwarts, C. M. G., Transmission line wave height transducer, in *Proceedings of the International Symposium on Ocean Wave Measurement and Analysis*, vol. 1, pp. 605-620, Am. Soc. Civ. Eng., New York, 1974.

T. A. Hardy, Department of Civil and Systems Engineering, James Cook University, Townsville, Queensland, 4811, Australia. (email: Thomas.Hardy@jcu.edu.au)

I. R. Young, Department of Civil Engineering, University College, University of New South Wales, Canberra, ACT 2600, Australia. (email: iry@waves.ce.adfa.oz.au)

(Received July 12, 1994; revised September 7, 1995; accepted November 22, 1995)